Research Square

Preprints are preliminary reports that have not undergone peer review.
They should not be considered conclusive, used to inform clinical practice,
or referenced by the media as validated information.

Integrated Static Reservoir Modelling and Uncertainty Hierarchy of Multi-Level Reservoirs in a Structurally Complex Faulted Systems: A Case Study of Albite Field

I Obihan

obihan.ifeanyi@yahoo.com

Salem University

O Ologe

Federal University Lokoja

T. S. Alege

Federal University Lokoja

I Abdulbariu

Federal University Lokoja

A. A. Ameloko

3 Department of Geosciences, Confluence University of Science and Technology Osara, Kogi State, Nigeria

Research Article

Keywords: Reservoir characterization, Static modelling, Reservoir connectivity, Depositional environment, Compartmentalization, Volumetric estimation and Uncertainty analysis

Posted Date: November 5th, 2026

DOI: https://doi.org/10.21203/rs.3.rs-11321637/v1

License: This work is licensed under a Creative Commons Attribution 4.0 International License.
Read Full License

Additional Declarations: No competing interests reported.

Integrated Static Reservoir Modelling and Uncertainty Hierarchy of Multi-Level Reservoirs in a Structurally Complex Faulted Systems: A Case Study of Albite Field

Obihan, I[1], Ologe O[2], Alege T.S[2] and Abdulbariu, I[2] Ameloko A, A[3]

[1] Department of Earth, Salem University. Lokoja, Kogi State, Nigeria

[2] Department of Geology, Federal University Lokoja, Kogi State, Nigeria

[3] Department of Geosciences, Confluence University of Science and Technology Osara, Kogi State, Nigeria

Corresponding Author email: obihan.ifeanyi@yahoo.com

Abstract

This study presents an integrated reservoir characterization and static modelling assessment of the B9300, H1400 and J9400 reservoirs in the Albite Field. Seismic interpretation, structural mapping, depositional analysis, facies and petrophysical modelling, fluid-contact evaluation, volumetric estimation and uncertainty analysis were combined to assess reservoir architecture, quality, connectivity and hydrocarbon potential. Structural interpretation revealed a fault-controlled system dominated by growth faults that govern trap formation, compartmentalization and fluid distribution. Depositional analysis showed a transition from high-energy fluvial channels in B9300, through mixed fluvio-tidal conditions in H1400, to marine-influenced, shale-rich settings in J9400, producing increasing heterogeneity and declining reservoir quality with depth. B9300 is sand-rich, with high porosity, permeability, net-to-gross and hydrocarbon saturation, and excellent lateral and vertical connectivity. H1400 holds significant hydrocarbon volumes but shows higher shale content, facies variability and fault-related compartmentalization, giving moderate quality and greater uncertainty. J9400 is shale-dominated, with low effective porosity and permeability, high water saturation and poor connectivity. Fluid-contact modelling confirmed structurally controlled accumulations, with B9300 displaying the most extensive and continuous hydrocarbon columns and H1400 and J9400 progressively smaller, more isolated accumulations. Volumetric analysis yielded P50 STOIIP estimates of about 550 MMstb (B9300), 860–900 MMstb (H1400) and 252 MMstb (J9400). Structural uncertainty was negligible, with volumetric variability controlled mainly by petrophysical properties, facies distribution and connectivity. B9300 is the most attractive development target, H1400 is volumetrically significant but moderately uncertain, and J9400 has limited economic potential. These results provide a framework for reservoir management, field development planning and future dynamic simulation.

Keywords: Reservoir characterization; Static modelling; Reservoir connectivity; Depositional environment; Compartmentalization; Volumetric estimation and Uncertainty analysis

,

1.1 Introduction

The Niger Delta Basin is one of the world's most prolific hydrocarbon provinces, containing a thick succession of Tertiary sediments deposited during the progradation of one of the largest regressive delta systems globally. The basin has accumulated more than 10 km of clastic sediments and hosts the highly productive Akata–Agbada petroleum system, where the Agbada Formation constitutes the principal hydrocarbon-bearing interval while the Akata Formation serves as the major source rock. The basin has undergone significant syn-sedimentary tectonic deformation characterized by growth faulting, rollover anticlines, shale mobilization, and structural compartmentalization, which collectively control hydrocarbon generation, migration, trapping, and reservoir distribution (Tuttle, et al., 1999).

Reservoirs within the Niger Delta are typically deposited in fluvial, deltaic, distributary channel, tidal, shoreface, and marine environments, resulting in substantial lateral and vertical heterogeneity in reservoir architecture. Variations in depositional energy, sediment supply, and accommodation space produce complex facies distributions that directly influence porosity, permeability, net-to-gross ratio (NTG), hydrocarbon saturation, and reservoir connectivity.

Previous studies have demonstrated that reservoir quality within Niger Delta fields is strongly controlled by depositional environment and facies architecture, with channelized sand bodies generally exhibiting superior reservoir properties compared to shale-dominated marine intervals (Nton et al., 2016). Accurate characterization of such complex reservoirs remains a fundamental challenge in field development and reservoir management. Traditional reservoir evaluation approaches based solely on well-log interpretation or structural mapping often fail to adequately capture the spatial variability of reservoir properties and the uncertainty associated with subsurface heterogeneity. Consequently, the petroleum industry has increasingly adopted integrated reservoir modelling approaches that combine seismic interpretation, facies analysis, petrophysical characterization, volumetric assessment, and uncertainty evaluation to improve subsurface understanding and reduce development risks. Studies conducted in several Niger Delta fields have shown that integrated static reservoir modelling provides a more realistic representation of reservoir architecture, fluid distribution, and reservoir performance than isolated geological or petrophysical analyses (Ikomi and Nfor, 2021). Static reservoir models form the foundation for reservoir management because they

provide a three-dimensional representation of structural geometry, facies distribution, petrophysical properties, fluid contacts, and hydrocarbon volumes.

These models are essential for calculating stock tank oil initially in place (STOIIP), evaluating reservoir connectivity, planning well locations, and supporting dynamic simulation studies. However, the reliability of reservoir models depends largely on how effectively geological complexity, property heterogeneity, and associated uncertainties are represented. Failure to adequately quantify uncertainty may result in biased volumetric estimates, misleading recoverable reserve assessments, and suboptimal field development decisions (Ikomi et al., 2021).

Recent advances in geostatistical modelling and uncertainty analysis have enabled reservoir characterization to move beyond deterministic interpretations toward probabilistic frameworks that explicitly account for geological uncertainty. In such frameworks, uncertainty may arise from multiple sources including structural interpretation, facies distribution, petrophysical property modelling, fluid-contact definition, reservoir connectivity, and volumetric estimation. While many studies in the Niger Delta have addressed individual aspects of reservoir characterization, relatively few have examined the hierarchical evolution of uncertainty across multiple vertically stacked reservoirs within the same structural framework. Consequently, understanding how uncertainty evolves between reservoirs of different depositional settings and qualities remains an important research challenge (Avbovbo., 1978).

1.2 Geologic Setting

The Albite Field is located within the Niger Delta Basin, one of the most prolific hydrocarbon provinces in the world. The basin developed on the passive continental margin of the Gulf of Guinea following the separation of the African and South American plates during the Late Jurassic to Early Cretaceous rifting event (Short and Stauble, 1967; Avbovbo, 1978). Subsequent thermal subsidence and rapid sediment supply from the Niger–Benue river system resulted in the accumulation of more than 10 km of Tertiary clastic sediments and the progressive south-westward progradation of the delta (Doust and Omatsola, 1990; Tuttle et al., 1999).

The paleogeography of the Niger Delta reflects a transition from continental fluvial environments in the north to marginal marine and deep-marine environments toward the south and offshore regions. Repeated fluctuations in sea level and sediment supply generated a variety of depositional systems, including fluvial channels, distributary channels, delta-front

sands, shoreface deposits, and marine shales, which collectively control reservoir architecture and heterogeneity throughout the basin (Doust and Omatsola, 1990; Abiola et al., 2018).

Structurally, the Niger Delta is characterized by gravity-driven tectonics associated with the loading of thick sedimentary sequences on over-pressured Akata shales. This process led to the development of listric growth faults, rollover anticlines, shale diapirs, and fault-related structural traps that constitute the principal hydrocarbon trapping mechanisms in the basin (Evamy et al., 1978; Doust and Omatsola, 1990).

The sandstone reservoirs serve as hydrocarbon-bearing zones, while the shale layers provide effective seals for petroleum accumulation. This stratigraphy aligns with the broader Niger Delta depositional environment**,** which has undergone significant geological evolution since the Paleogene (Obaje, 2009). The Niger Delta Basin, among the world's largest Tertiary deltas, remains a highly prospective hydrocarbon system despite its maturity (Tsimitakopoulos, 2022). Its development is shaped by southwestern winds and longshore currents, which initiated various depositional events in the early Tertiary. Sediment deposition primarily occurs along barrier bar fronts**,** while minor portions migrate downslope via submarine channels (Burke, 1972).

The Albite Field exhibits these typical Niger Delta structural styles, with fault-controlled compartmentalization significantly influencing reservoir distribution and connectivity. The stratigraphic succession of the Niger Delta comprises three major lithostratigraphic units: the Akata, Agbada, and Benin formations. The Akata Formation consists predominantly of deep-marine shales and serves as the principal source rock, while the overlying Agbada Formation comprises alternating sandstone and shale sequences that host the majority of the basin's hydrocarbon reservoirs (Avbovbo, 1978; Tuttle et al., 1999). The uppermost Benin Formation consists mainly of continental sands deposited in fluvial environments (Short and Stauble, 1967).

1.3 Location of the Study Area

The study area, Albite field lies 50 kilometres Southwest of Port Harcourt in the onshore Eastern delta. The field is located within OML 25, and the block is located in the mangrove coastal swamp which extends slightly offshore. It is intersected by the San Bartholomeo River, which are large deltaic tidal channels that enter the Gulf of Guinea. The riverine and swamp environment makes for difficult operating conditions. The field is between Latitudes ~4°30′N

to 4°33′N and Longitude: ~6°33′E to 6°36′E and covers an area of approximately 399.8 km^2 (Fig. 1).

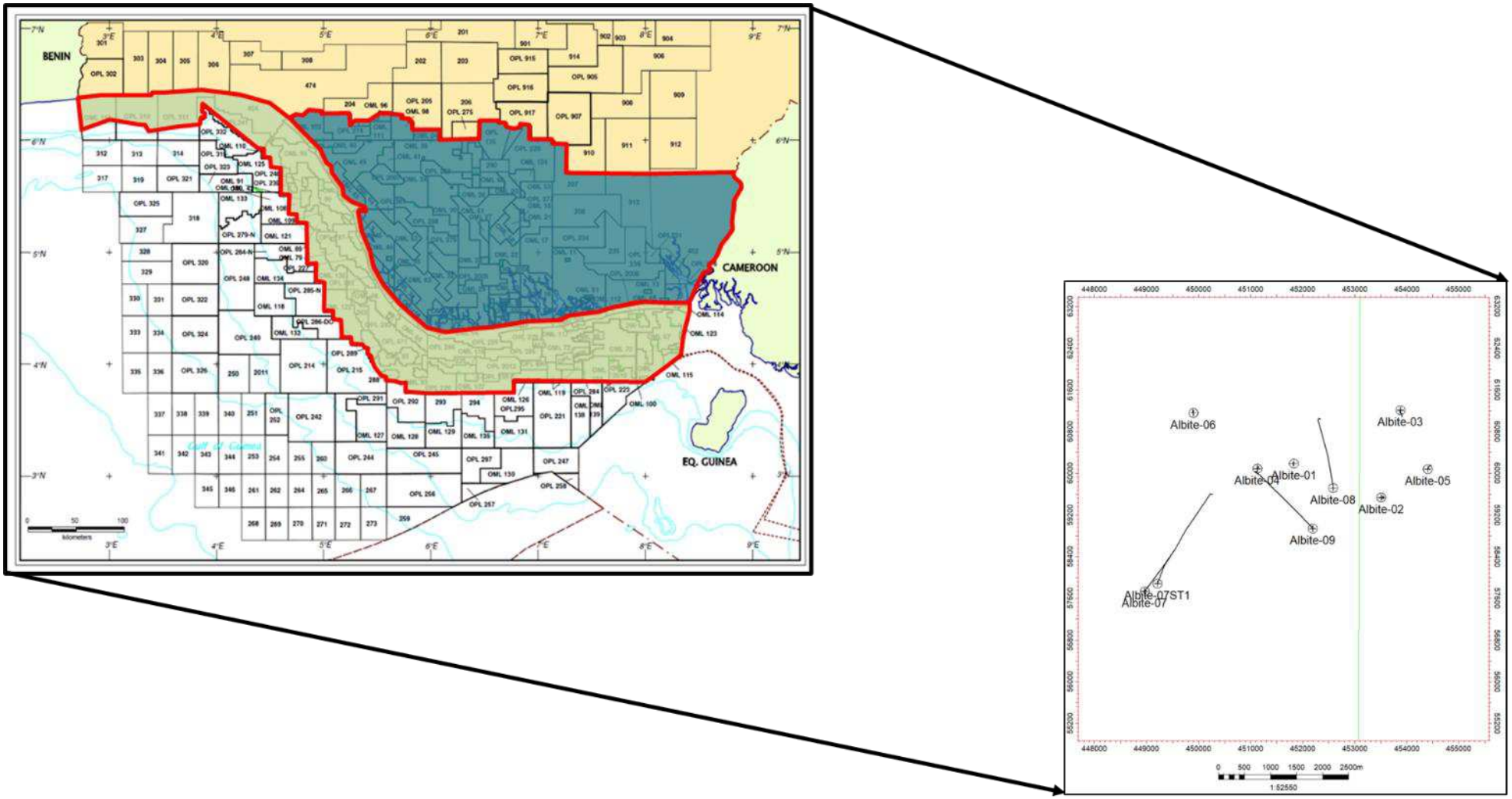


Fig. 1-Map Showing the Location of Wells used in Albite Field

2.1 Methodology

Data was QCed properly, sorted into formats compatible with Schlumberger PETREL^{TM} 2024 and loaded into the software for analysis. Well logs were edited, normalized, depth matched, and checked for consistency. The seismic data were conditioned to ensure continuity of reflectors and improved fault identification. This study employed an integrated static reservoir modelling workflow to characterize the three (3) reservoirs within the Albite Field, Niger Delta. The workflow incorporated 3D seismic data, well logs, well tops, check-shot surveys, and seismic data.

Well-log correlation was first carried out to delineate reservoir intervals and establish stratigraphic continuity across the field. Structural interpretation of seismic data was then performed to identify faults, map reservoir horizons, and define the structural framework controlling hydrocarbon accumulation. Seismic horizons were converted from time to depth using well velocity (checkshot). Subsequently, seismic attribute analyses, RMS amplitude including were conducted to delineate depositional channel systems, reservoir fairways, and potential hydrocarbon-bearing zones.

These results were integrated with well-log responses to determine the depositional environments of the reservoirs, which ranged from fluvial through fluvio-tidal to marine-influenced settings. A three-dimensional structural framework was generated through pillar gridding, zonation, and layering.

Facies modelling was performed using Sequential Indicator Simulation (SIS) to distribute sand and shale facies within the reservoir grid, while petrophysical properties including volume of shale (Vsh), total porosity (PHIT), effective porosity (PHIE), water saturation (Sw), permeability (K), and net-to-gross ratio (NTG) were modelled using geostatistical techniques. Oil–water contacts were subsequently defined, and fluid distribution models were generated to assess reservoir connectivity and hydrocarbon column geometry.

Volumetric analysis was conducted using static reservoir models to estimate Stock Tank Oil Initially in Place (STOIIP) for each reservoir. To evaluate model reliability and development risk, uncertainty analysis was performed using multiple reservoir realizations and a probabilistic framework comprising P10, P50, and P90 scenarios. Finally, all structural, depositional, petrophysical, fluid-contact, volumetric, and uncertainty results were integrated to establish a reservoir ranking and uncertainty hierarchy, identifying B9300 as the highest-quality, lowest-risk reservoir, H1400 as a moderately heterogeneous reservoir, and J9400 as a

geologically constrained, high-uncertainty reservoir. This integrated workflow was utilized to carry out this project as shown below in Fig. 2.

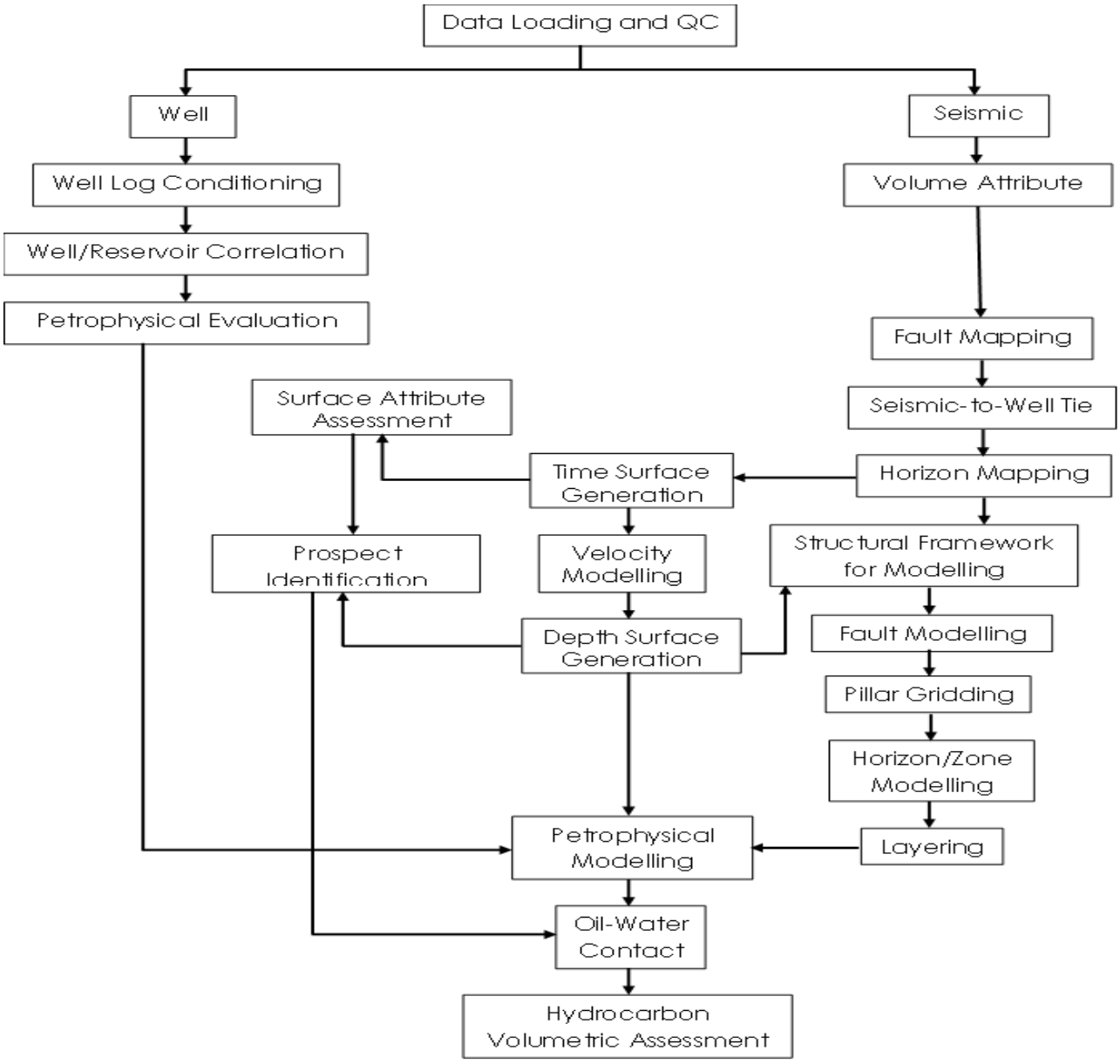


Fig. 2-An Integrated Workflow Utilized to Execute the Study.

This study adopted an integrated static reservoir characterization workflow that combines structural interpretation, petrophysical analysis, facies modelling, property population, volumetric estimation, and a tiered (hierarchical) uncertainty analysis. The workflow was designed specifically to address the compounding sources of uncertainty that arise in structurally complex, multi-fault, multi-reservoir settings such as the Albite Field, where reservoir compartmentalization, fault-seal behaviour, and vertical stacking of sand bodies

introduce uncertainty at several independent levels (structural, stratigraphic, petrophysical, and volumetric).

3.1 Result and Observation

3.1.1 Stratigraphic Correlation

The lithostratigraphic correlation panel (A–A′) illustrates a detailed well-to-well correlation across the Albite Field, integrating gamma ray, resistivity, density, and neutron log responses. The correlation section spans multiple wells arranged along a structural cross-section, with the well locations and orientation shown in the inset map. This arrangement ensures that stratigraphic relationships are evaluated in their correct spatial and structural context rather than as isolated vertical profiles (Fig. 3).

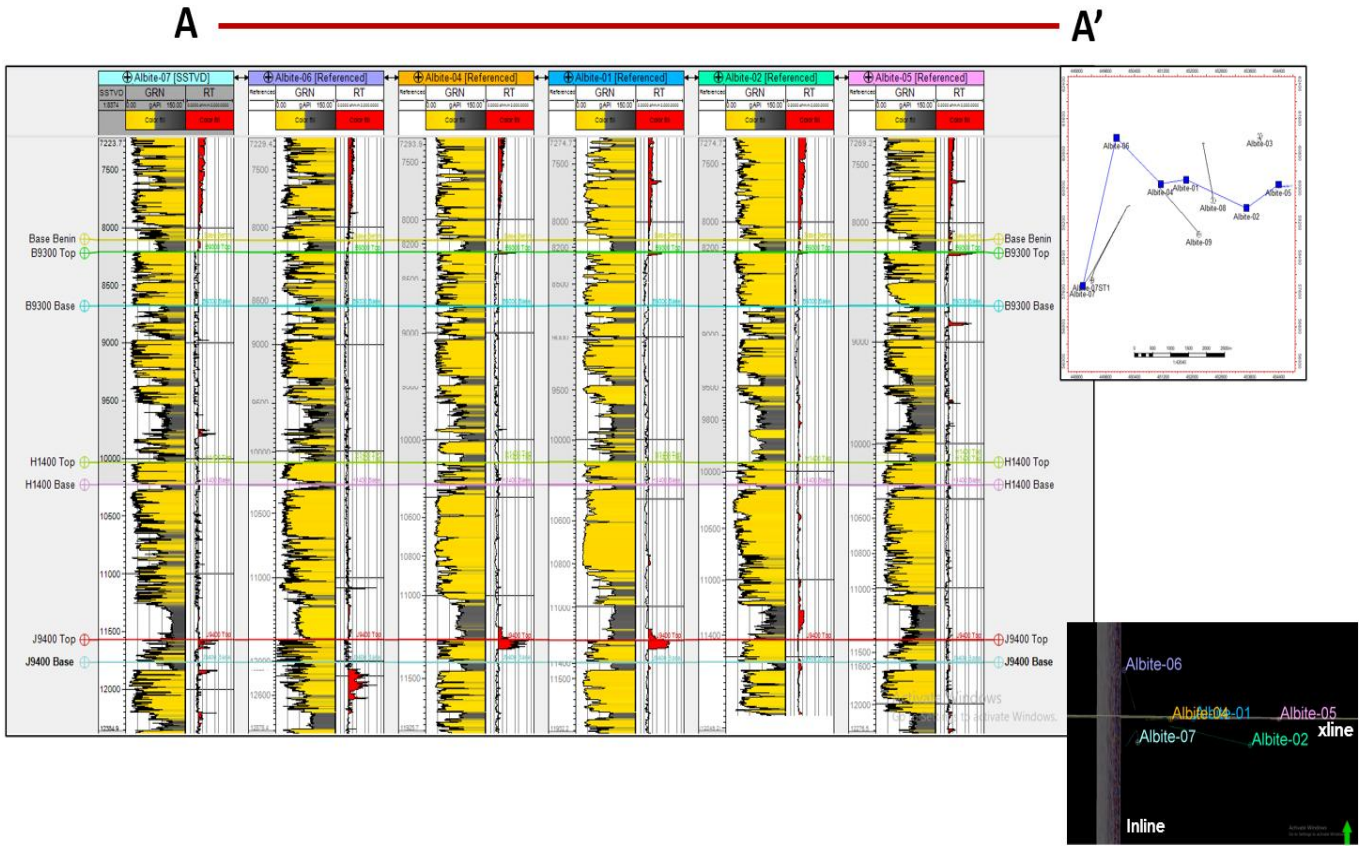


Fig. 3-Lithostratigraphy Correlation (xline Direction)

Across the section, several laterally persistent stratigraphic markers are identified and labeled (e.g., Base and Top of key sand packages). These markers define distinct stratigraphic intervals that can be traced with a high degree of confidence between wells, indicating good stratigraphic

continuity within the field. The consistency of log motifs, particularly the blocky to bell-shaped gamma ray signatures highlighted in yellow, suggests repeated deposition of sand-dominated units separated by shale intervals (Fig. 4). These sands are interpreted as reservoir units, while the intervening shale units act as intra-reservoir baffles or seals. The synthetic seismograms was generated using calibrated sonic and density logs and are directly compared with the extracted seismic traces (Fig. 5). Overall, a good correlation is observed between the synthetic and real seismic responses across the three wells, indicating that the impedance contrasts derived from the well logs successfully reproduce the primary seismic reflection character.

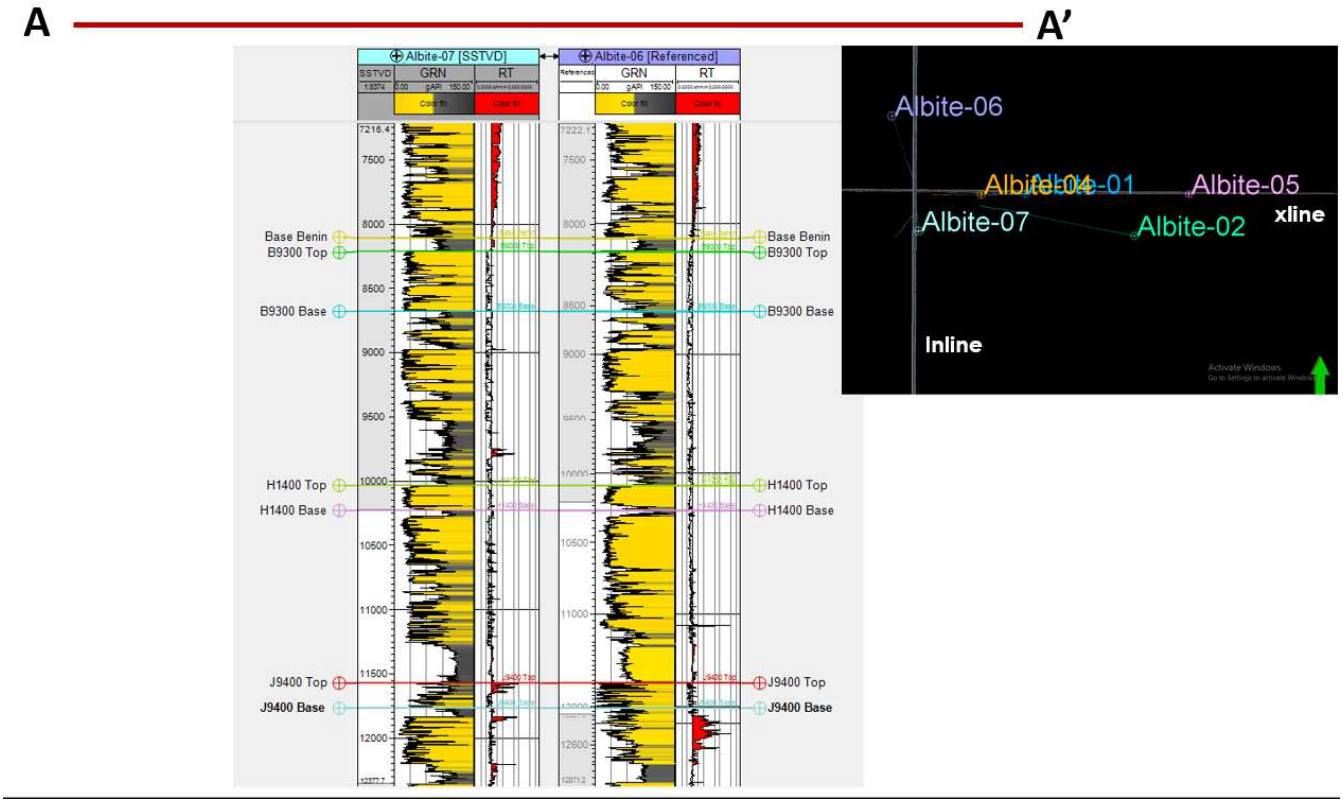


Fig. 4- Lithostratigraphy Correlation (inline Direction)

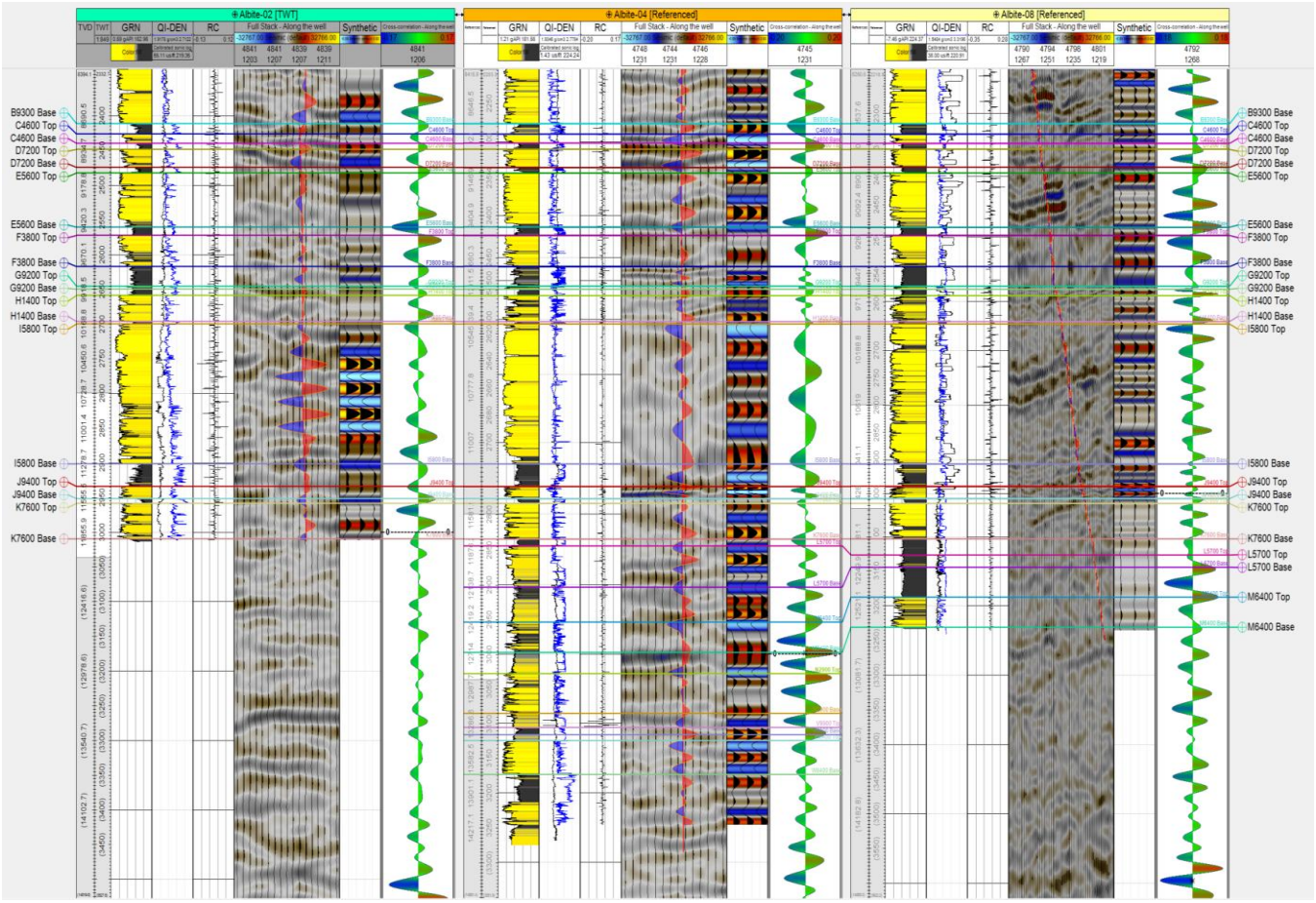


Fig. 5-Multi Well Synthetic Seismogram for Albite 02, 04 and 08 Wells

Major reflection peaks and troughs in the synthetic traces align well with those observed in the seismic data, particularly at the tops and bases of prominent reservoir units. This alignment confirms that the wavelet and time–depth relationships applied during the calibration are appropriate for the field.

3.1.2 Environment of Deposition

The EOD interpretation of Albite-02 indicates a progressive depositional transition from fluvial channel sands in B9300, through mixed fluvio-tidal deposits in H1400, to marine-influenced, shale-rich facies in J9400. B9300 is characterized by thick, laterally continuous channel sands with excellent reservoir quality and connectivity, whereas H1400 exhibits increased facies variability and heterogeneity due to the influence of tidal and deltaic processes. J9400 contains predominantly tidal, fluvio-deltaic, and marine shale facies with thinner, compartmentalized sand bodies and poor reservoir continuity (Fig. 6). This upward-to-downward transition reflects a retro gradational depositional trend, with increasing shale content and decreasing depositional

energy, explaining the observed decline in reservoir quality, connectivity, and hydrocarbon potential from B9300 to J9400.

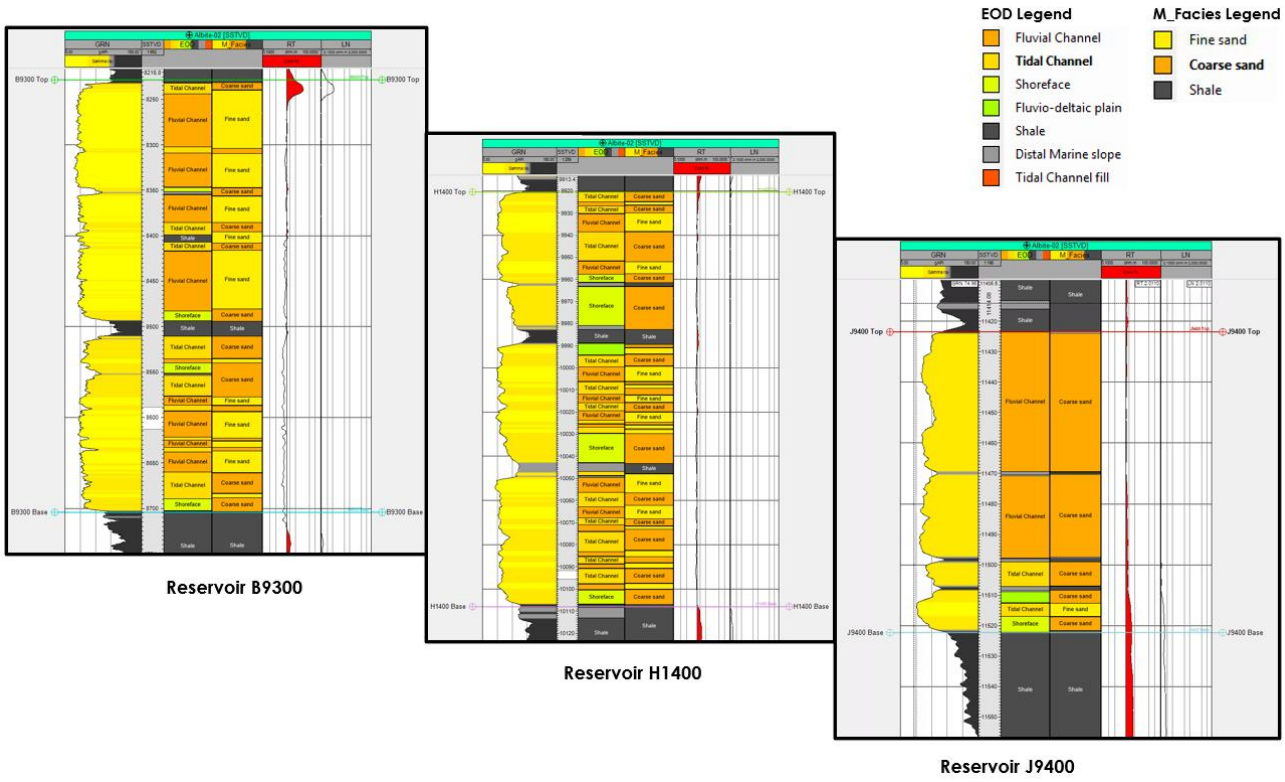


Fig. 6- Environment of Deposition Interpretation for Albite-02

The Environment of Deposition (EOD) interpretation of Albite-04 demonstrates a clear vertical transition from fluvial-dominated channel deposits in B9300, through heterogeneous fluvio-tidal deposits in H1400, to marine-influenced, shale-rich facies in J9400. The B9300 reservoir is characterized by thick, stacked fluvial channel sands with excellent continuity and reservoir quality, while H1400 exhibits increased facies variability due to the incorporation of tidal channels, shoreface, and fluvio-deltaic deposits, resulting in greater heterogeneity and localized compartmentalization (Fig. 7). The J9400 reservoir contains predominantly tidal channel fill, fluvio-deltaic plain, marine slope, and shale facies, with thinner and less connected sand bodies indicative of stronger marine influence and reduced depositional energy.

Albite-08 indicates a progressive depositional transition from fluvial channel-dominated sands in B9300, through heterogeneous fluvio-tidal deposits in H1400, to marine-influenced and shale-rich facies in J9400. The B9300 reservoir comprises thick, laterally continuous channel sands deposited under high-energy fluvial conditions, resulting in excellent reservoir continuity

and connectivity. In contrast, H1400 is characterized by alternating fluvial, tidal, and fluvio-deltaic deposits, reflecting increasing marine influence and leading to greater facies variability, thinner sand bodies, and moderate compartmentalization. The J9400 reservoir contains predominantly tidal channel fill, fluvio-deltaic plain, marine slope, and shale facies, with thin, discontinuous sand bodies and poor connectivity (Fig. 8).

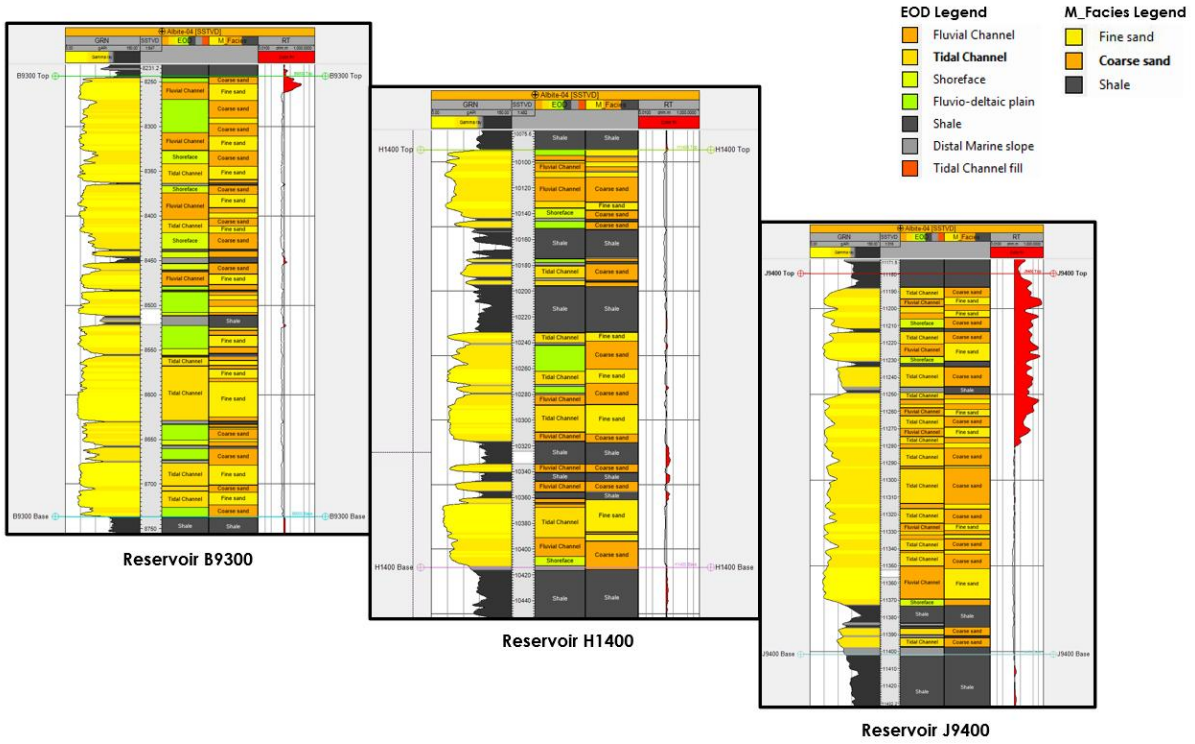


Fig. 7- Environment of Deposition Interpretation for Albite-04

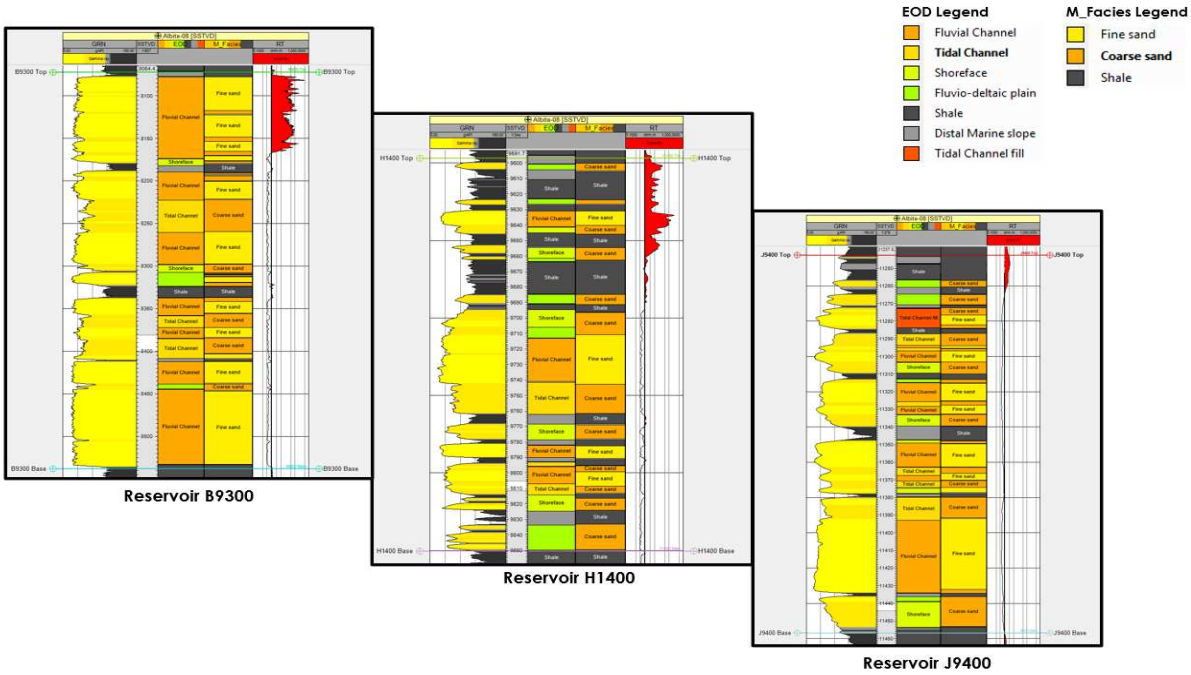


Fig. 8- Environment of Deposition Interpretation for Albite-08

3.1.3 Structural Interpretation

The Albite Field exhibits a complex fault-controlled structural framework dominated by multiple listric normal faults (F1 – F15) that segment the sedimentary succession into distinct fault blocks. Major structure-building faults, notably F1, F2, F7, F11, F12, and F15, create significant structural relief and define the primary trapping architecture of the field. Numerous synthetic and antithetic faults further compartmentalize the reservoirs, potentially reducing lateral and vertical connectivity. Reflector thickening toward major faults, particularly near F1 and F2, provides clear evidence of syn-sedimentary growth faulting, indicating active fault movement during deposition. These growth structures generated localized accommodation spaces that influenced sand distribution and reservoir thickness development.

The field architecture is therefore strongly controlled by fault-related deformation, which governs reservoir geometry, hydrocarbon migration pathways, and trap formation. Well locations are concentrated around structurally elevated fault blocks, suggesting targeting of favorable closure structures with reduced drilling risk. However, deeper downthrown compartments remain less penetrated, contributing to structural and volumetric uncertainty (Fig. 9). The seismic horizon interpretation of the Albite Field identified three major reservoir horizons (B9300_TVD, H1400_TVD, and J9400_TVD) within a structurally complex, fault-controlled setting. The horizons are traced as laterally continuous reflectors, with B9300

exhibiting the highest continuity, H1400 showing moderate continuity and localized heterogeneity, and J9400 displaying reduced continuity and greater structural deformation.

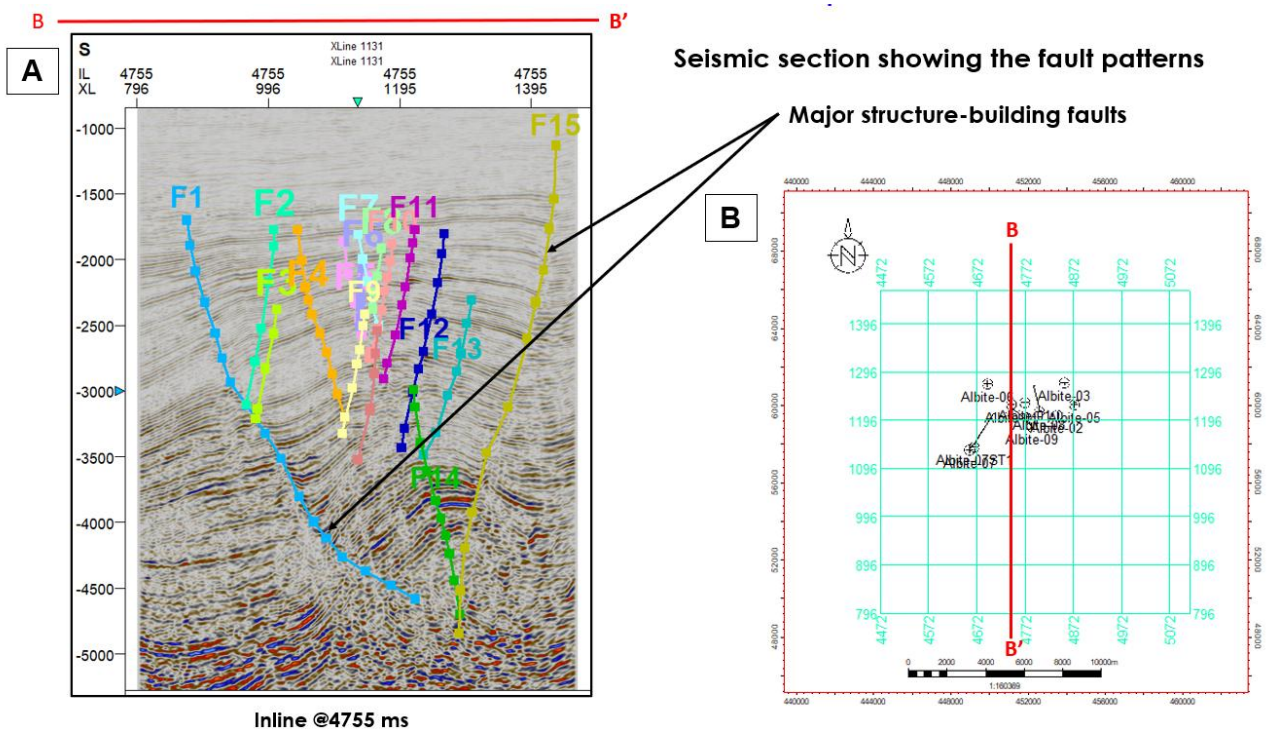


Fig. 9- Structural Framework – Fault Interpretation

Numerous normal growth faults offset all three horizons, with fault displacement increasing with depth, indicating syn-sedimentary fault activity and associated rollover structures. These faults divide the reservoirs into multiple compartments, influencing reservoir connectivity and hydrocarbon distribution. Structurally, the horizons form a central fault-bounded high flanked by downthrown blocks, creating potential structural traps and fault-assisted closures. The combined effects of faulting, reflector deformation, and increasing stratigraphic complexity with depth contribute significantly to reservoir compartmentalization and uncertainty, particularly within the deeper J9400 interval (Fig. 10).

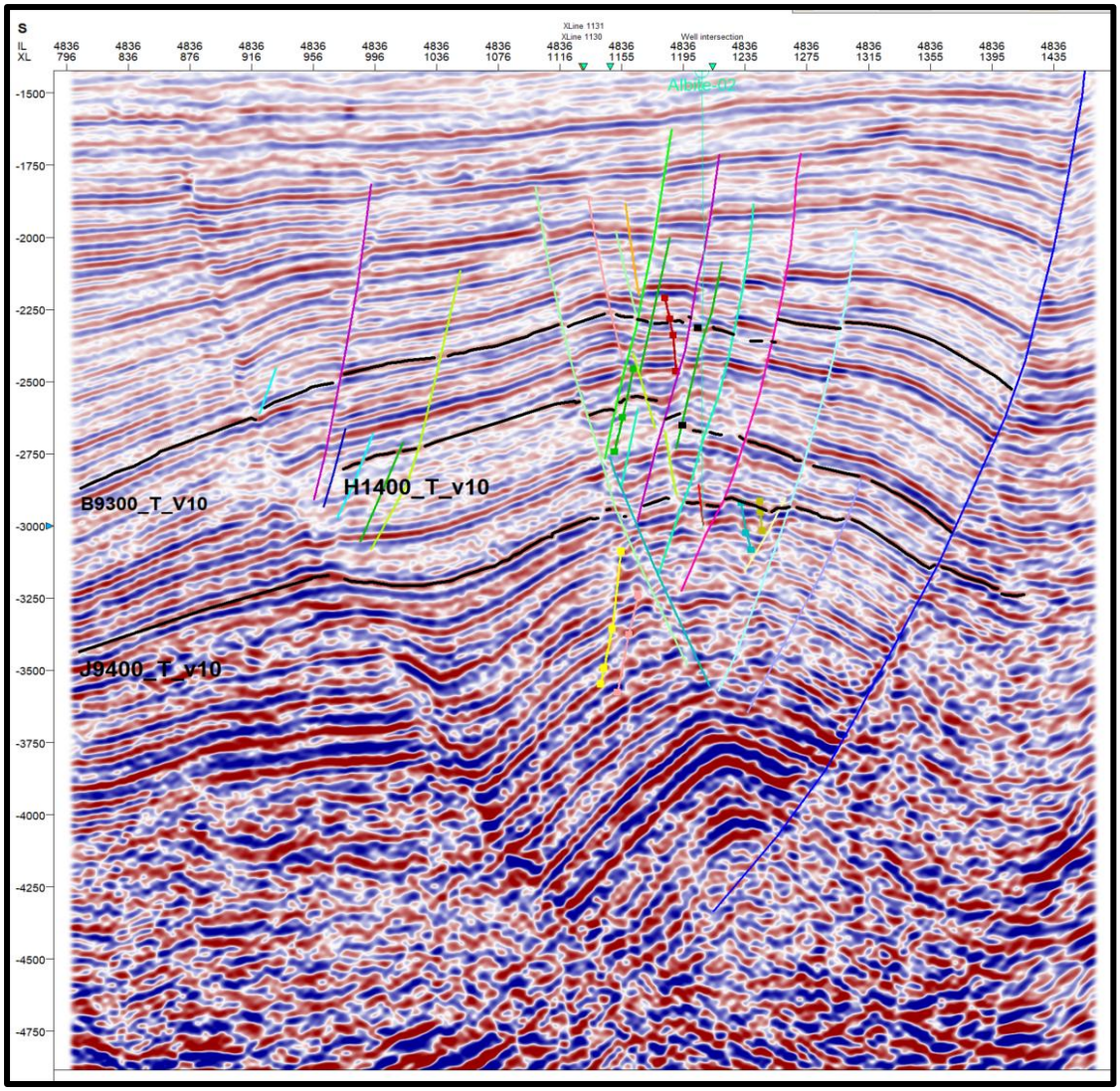


Fig. 10- Structural Framework - Horizon Interpretation

The B9300 fault polygons and top surface map reveal a fault-controlled reservoir architecture dominated by NE–SW to ENE–WSW trending growth faults within an extensional tectonic setting. The close correspondence between fault traces and contour offsets confirms that faulting exerts a primary control on the geometry of the B9300 horizon. The H1400 fault polygon and top surface maps reveal a structurally complex reservoir characterized by a dense network of NE–SW to ENE–WSW trending growth faults that exert strong control on reservoir geometry and compartmentalization. The close correlation between fault traces and contour offsets confirms that faulting is the primary control on the H1400 structural configuration. Compared to the B9300 and H1400 horizons, the J9400 level exhibits the greatest fault

continuity, displacement, and structural complexity, resulting in pronounced contour offsets and distinct fault-bounded compartments (Fig. 11).

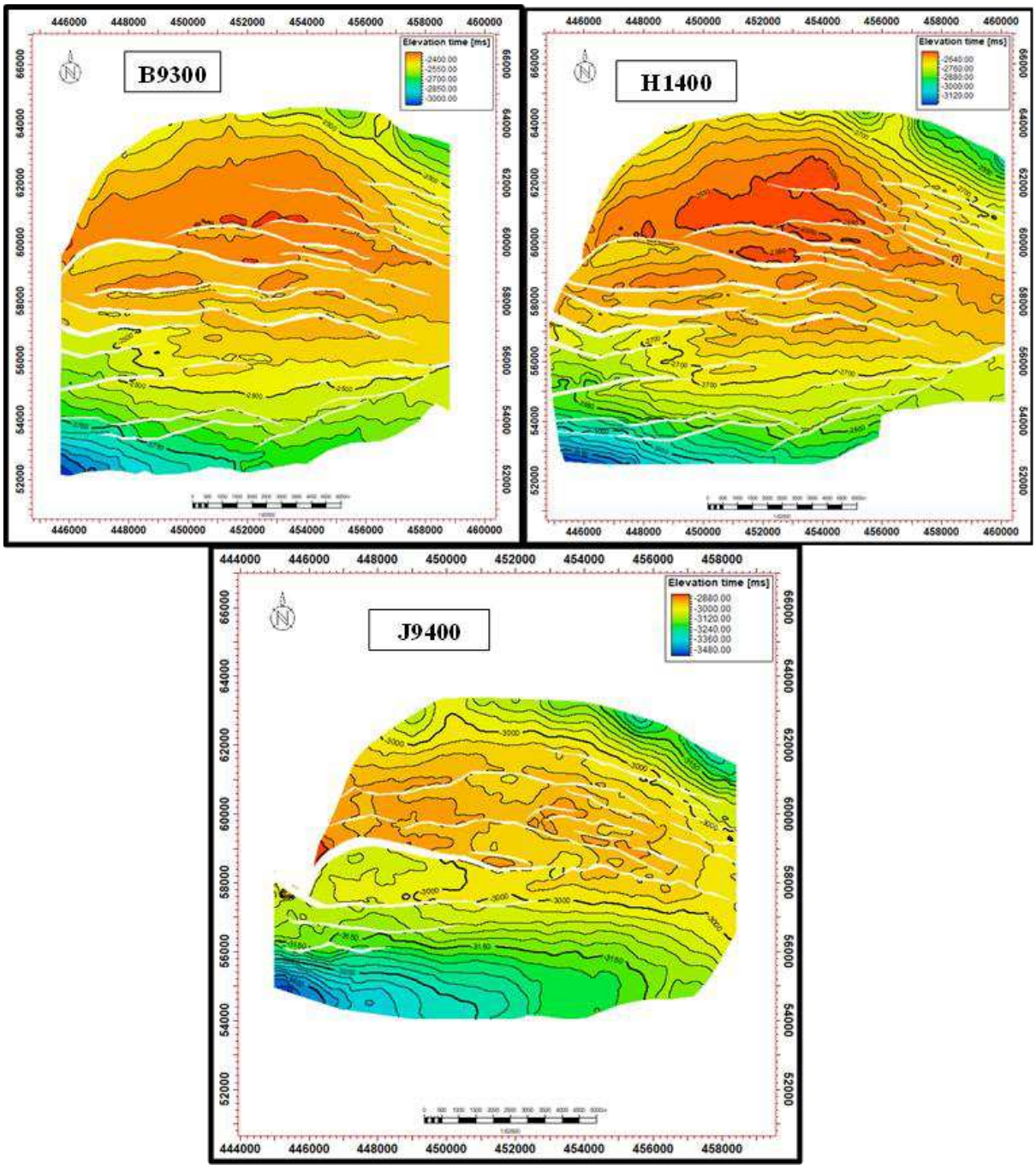


Fig. 11- B9300, H1400, and J9400 Interpreted Faulted Surfaces

3.1.4 Amplitude Attribute

The B9300 RMS Amplitude Attribute Map reveals a heterogeneous distribution of seismic amplitudes, with high-amplitude anomalies concentrated mainly within the Central and Northern parts of the field and lower amplitudes occurring toward the Southern and peripheral areas. Localized high-amplitude zones in H1400 were interpreted as relatively clean, fluvial or tidally reworked channel sands, while extensive low-amplitude areas likely represent shale-rich, heterolithic, or water-bearing intervals. The J9400 RMS Amplitude Attribute Map is dominated by low-to-moderate amplitude responses, indicating a shale-rich and highly heterogeneous reservoir with limited acoustic impedance contrast (Fig. 12). EOD modelling indicates a clear depositional evolution from a fluvial channel-dominated, sand-rich and highly connected B9300 reservoir, through a heterogeneous fluvio-tidal H1400 reservoir, to a marine-influenced, shale-dominated and highly compartmentalized J9400 reservoir, reflecting progressive reduction in depositional energy, sand continuity, reservoir quality, and connectivity with depth (Fig. 13).

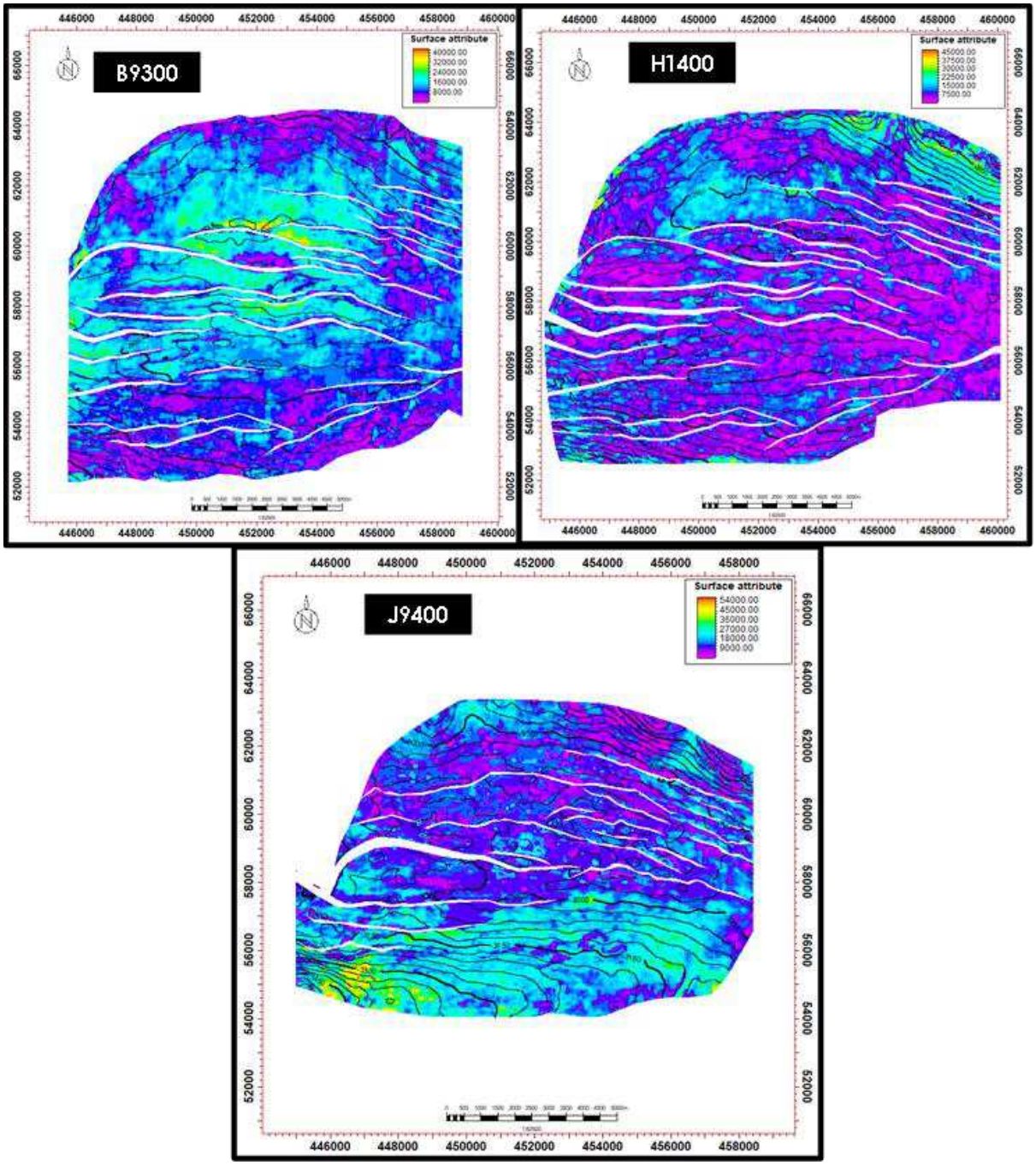


Fig. 12- RMS Amplitude Extracted for B9300, H1400, and J9400

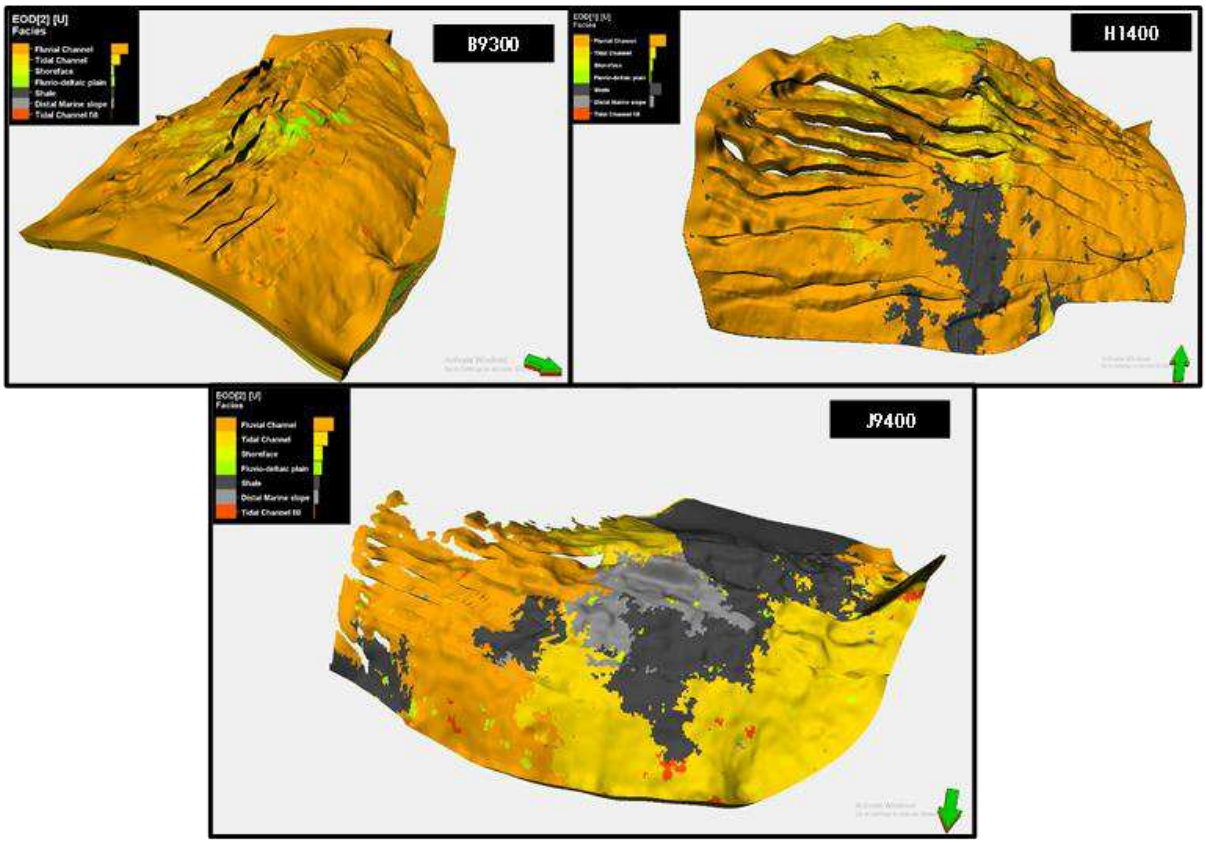


Fig. 13- Environment of Deposition Modelled for B9300, H1400, and J9400

3.1.5 Petrophysical and Fluid Contact Models

Facies modelling reveals a progressive deterioration in reservoir architecture from the sand-rich, highly connected fluvial B9300 reservoir, through the moderately heterogeneous and compartmentalized fluvio-tidal H1400 reservoir, to the shale-dominated, structurally controlled J9400 reservoir characterized by isolated sand bodies, poor connectivity, and high uncertainty (Fig. 14).

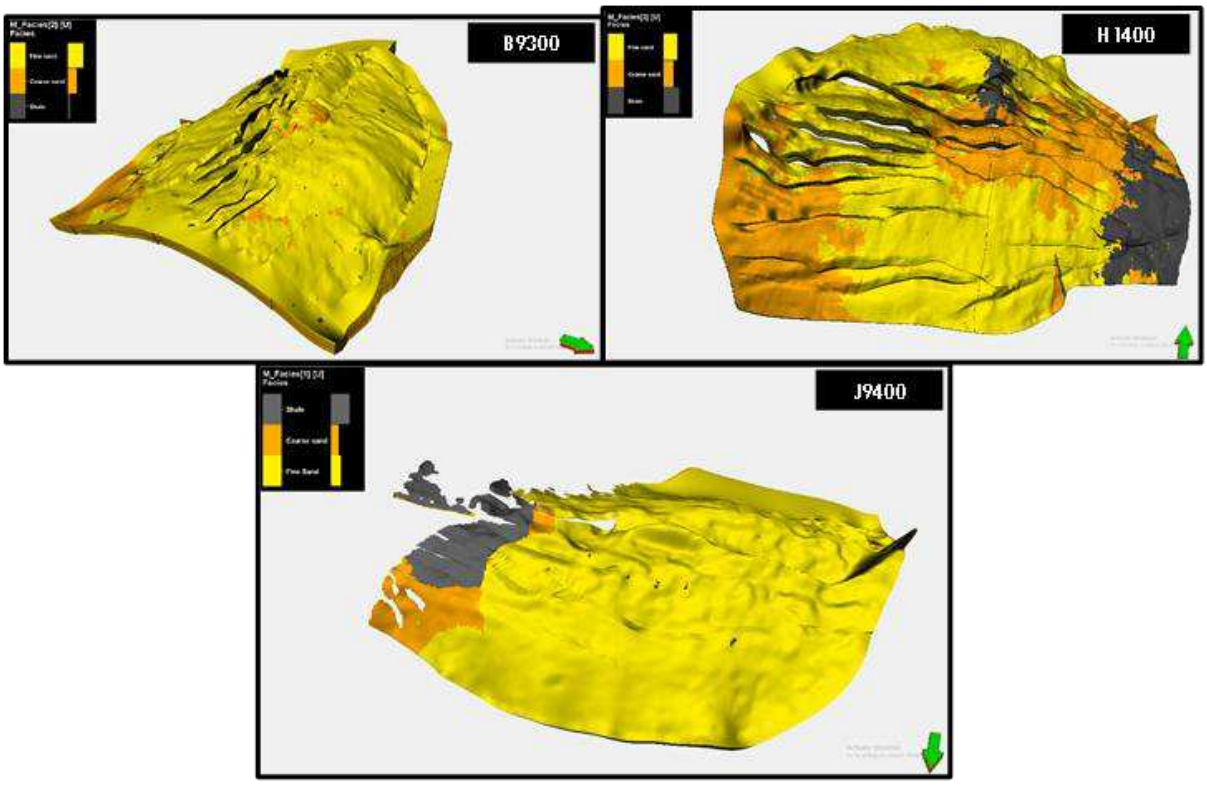


Fig. 14- Facies Modelling for B9300, H1400, and J9400

The total porosity (PHIT) models reveal a systematic depth-dependent decline in reservoir quality, with B9300 exhibiting high and laterally continuous porosity within sand-rich fluvial deposits, H1400 showing moderate and heterogeneous porosity controlled by fluvio-tidal facies and faulting, and J9400 displaying predominantly low porosity, strong shale influence, poor connectivity, and pronounced structural compartmentalization (Fig. 15). The effective porosity (PHIE) models demonstrate a progressive decline in effective reservoir quality with depth, with B9300 exhibiting high and well-connected effective porosity, H1400 showing moderate and facies-controlled effective porosity with increased compartmentalization, and J9400 characterized by low effective porosity, poor connectivity, dominant shale influence, and strong fault-controlled heterogeneity, confirming a depth-dependent deterioration in storage and flow capacity across the Albite Field (Fig. 16).

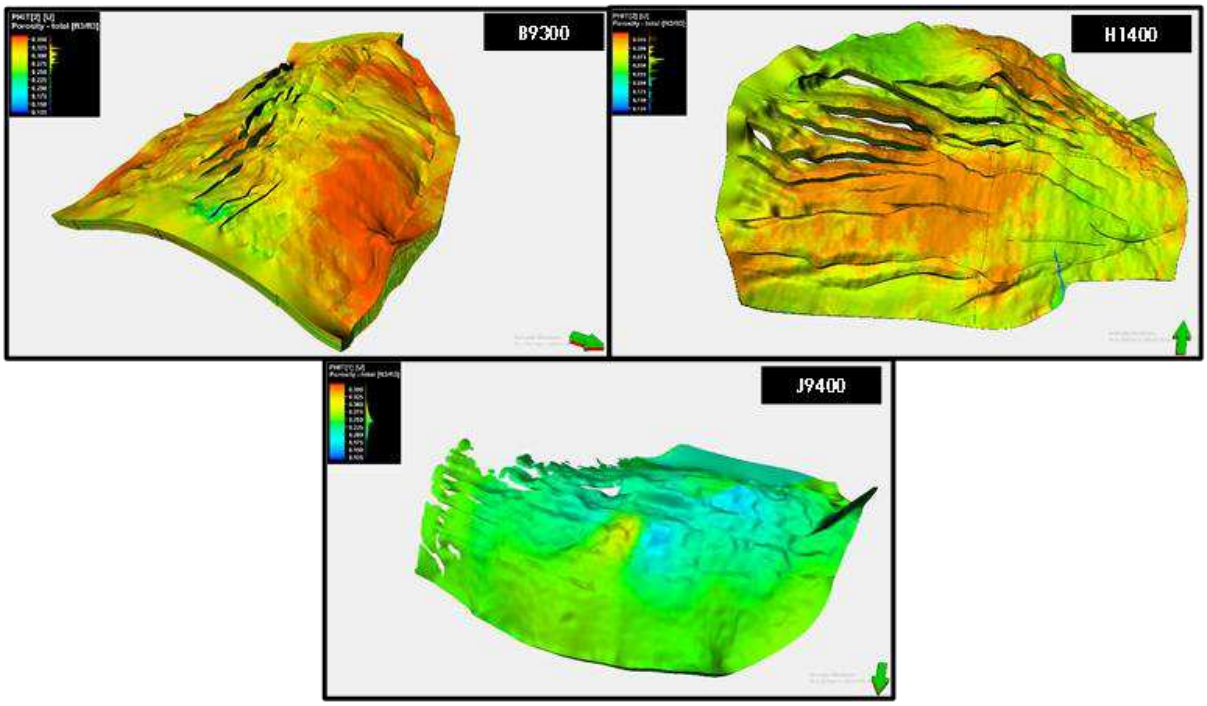


Fig. 15- Total Porosity Modelling for B9300, H1400, and J9400

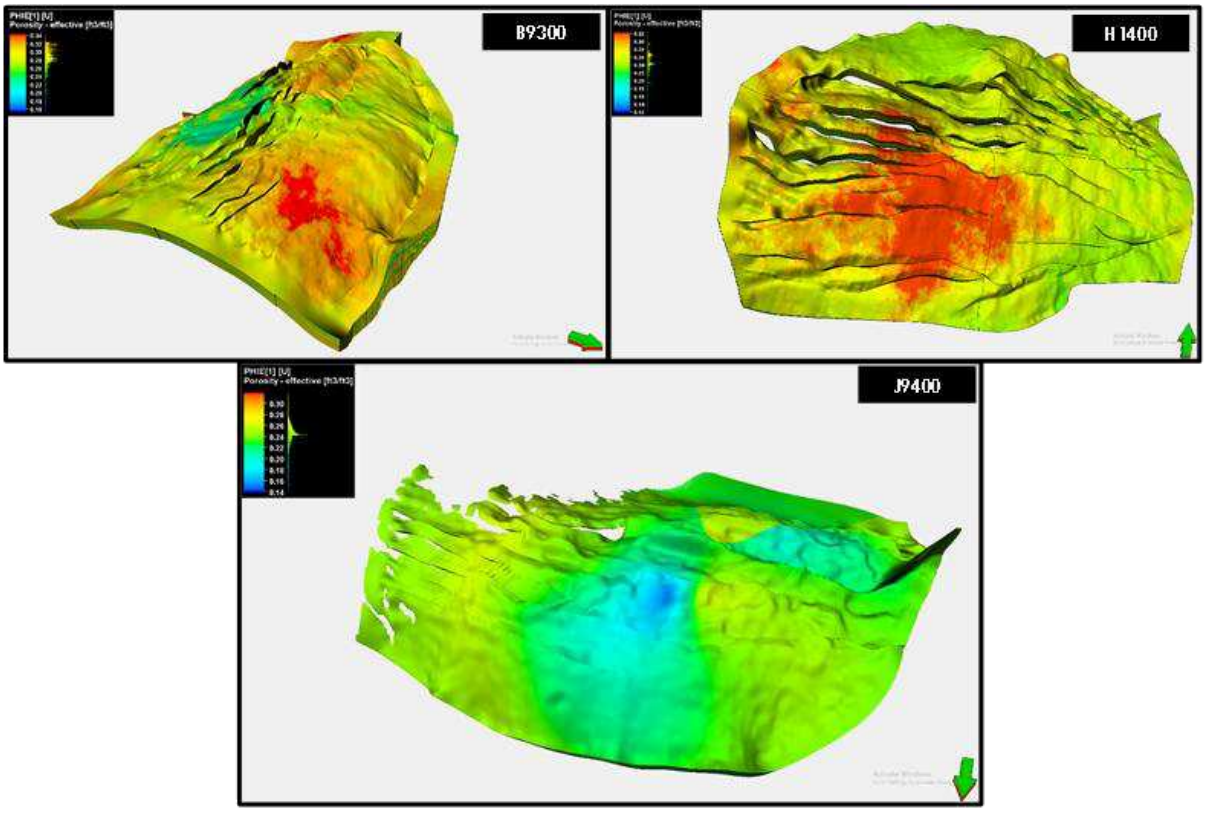


Fig. 16- Effective Porosity Modelling for B9300, H1400, and J9400

The shale volume (Vsh) models indicate a progressive increase in shale content with depth, from the clean, sand-dominated B9300 reservoir with minimal shale influence and excellent connectivity, through the moderately heterogeneous H1400 reservoir with significant shale-related compartmentalization, to the shale-dominated J9400 reservoir where extensive and vertically persistent mudstones severely reduce reservoir quality, connectivity, and volumetric certainty (Fig. 17).

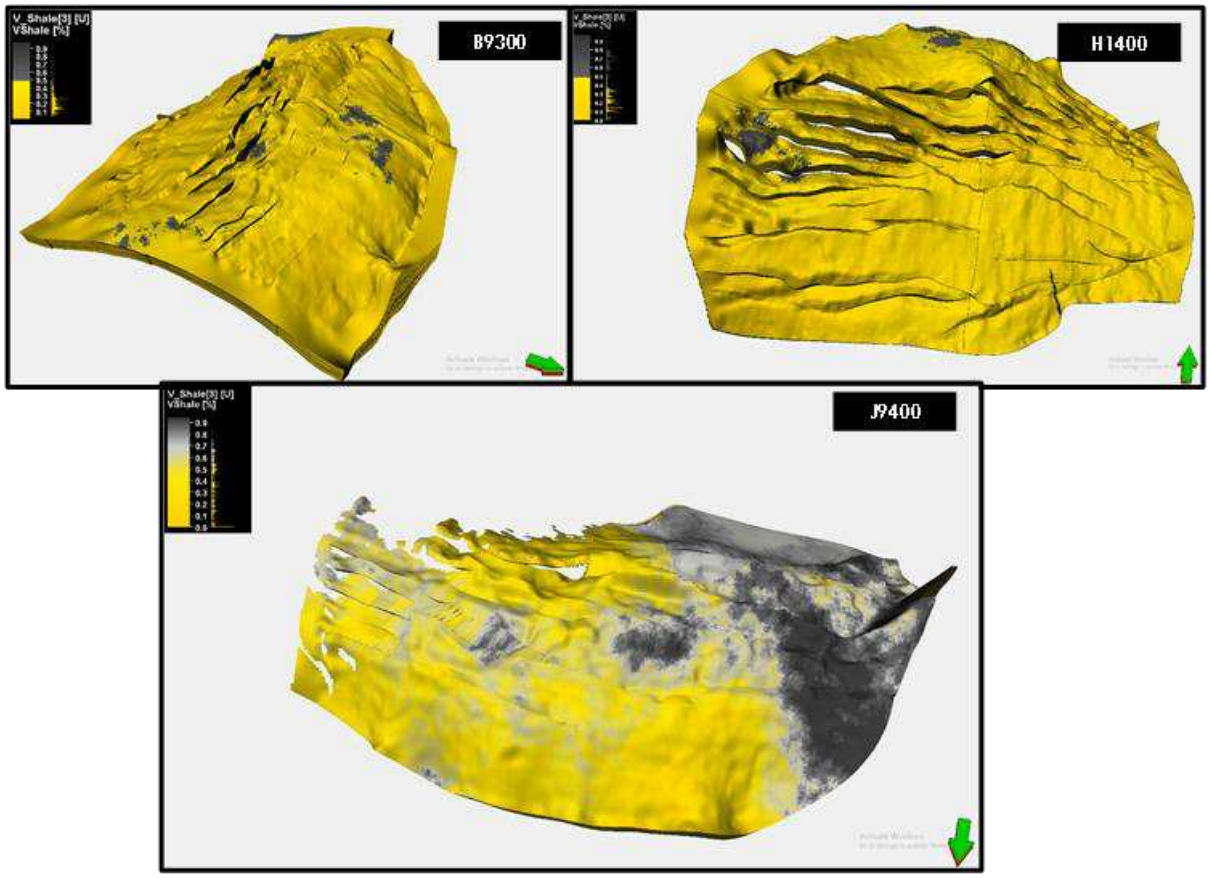


Fig. 17- Effective Porosity Modelling for B9300, H1400, and J9400

The water saturation (Sw) models show a progressive decline in hydrocarbon saturation with depth, with B9300 exhibiting low water saturation and extensive hydrocarbon fairways, H1400 displaying moderate and compartmentalized hydrocarbon accumulations, and J9400 characterized by predominantly high water saturation, isolated hydrocarbon pockets, poor connectivity, and strong fault-controlled fluid segregation, reflecting increasing shale content and reservoir degradation downward through the succession (Fig. 18).

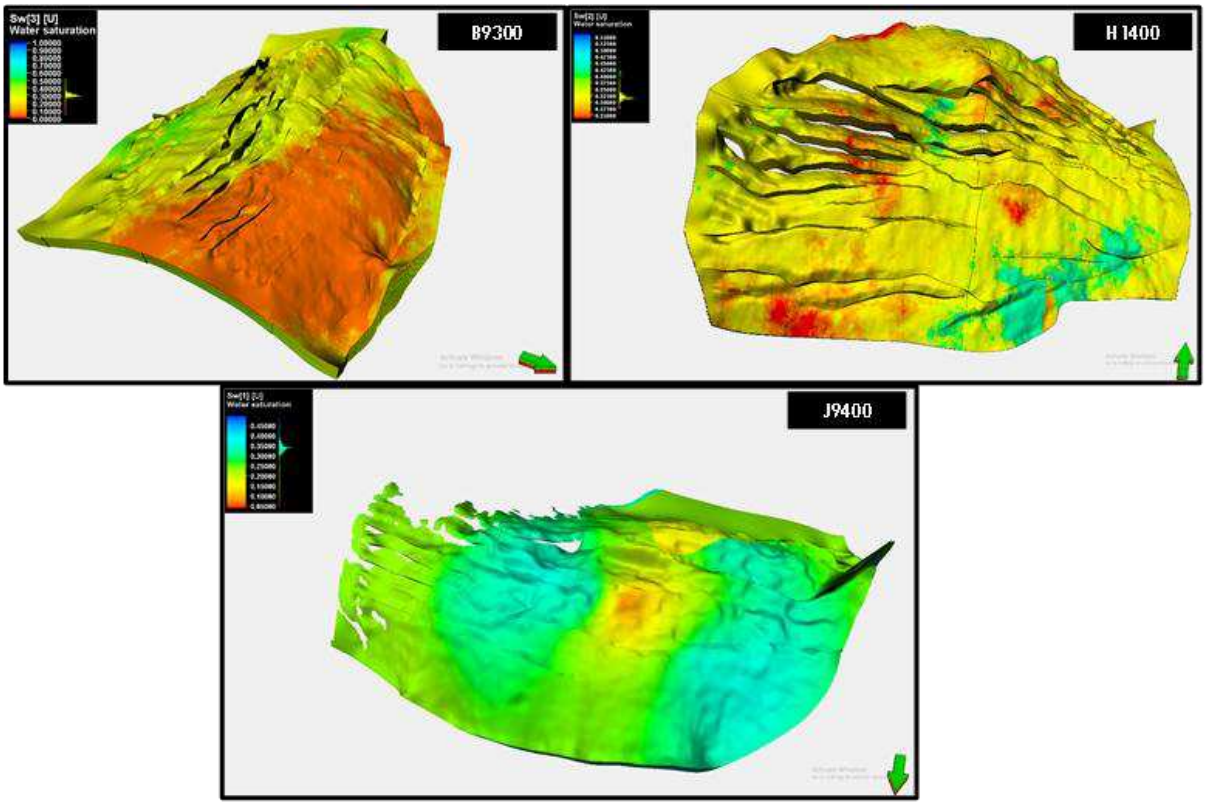


Fig. 18- Water Saturation Modelling for B9300, H1400, and J9400

The Net-To-Gross (NTG) models demonstrate a progressive decline in reservoir quality with depth, where B9300 exhibits high NTG values, laterally continuous sand bodies, and excellent reservoir connectivity; H1400 shows moderate and heterogeneous NTG controlled by fluvio-tidal facies and fault compartmentalization; while J9400 is characterized by low NTG, extensive shale dominance, poor net reservoir continuity, and highly localized reservoir development, reflecting increasing depositional and structural complexity downward through the succession (Fig. 19).

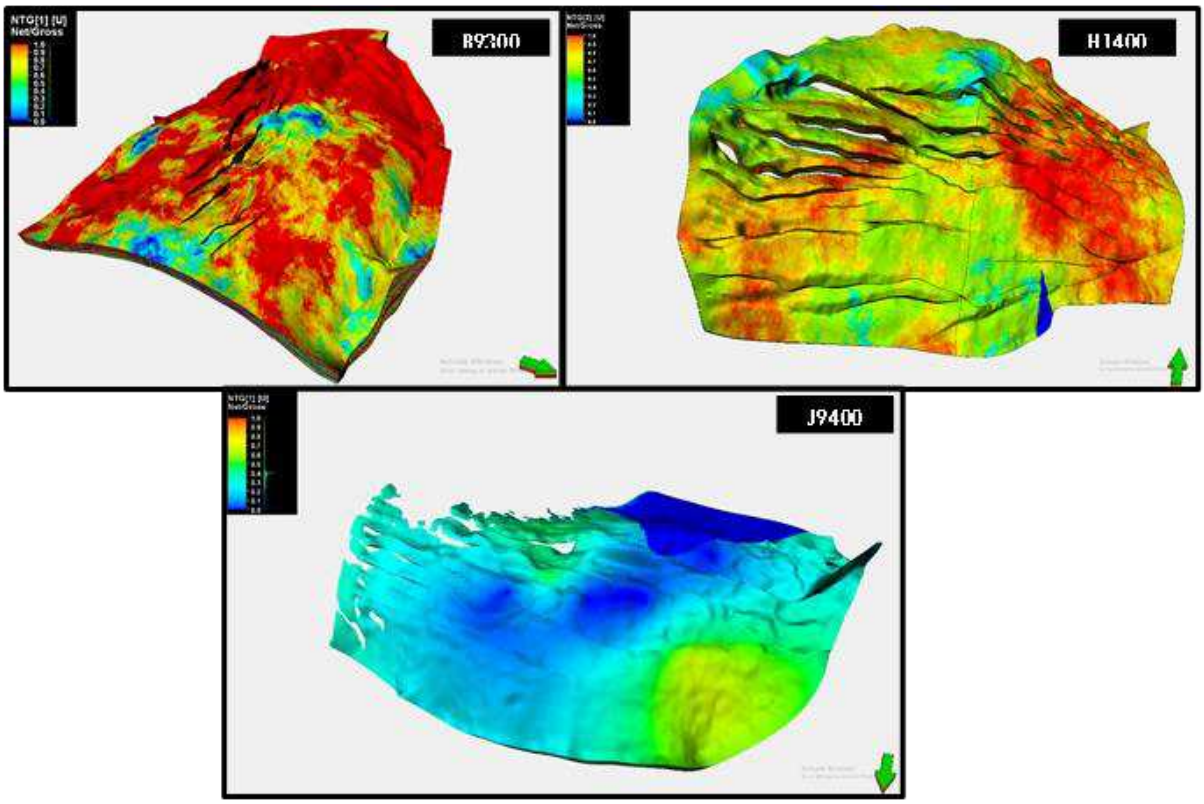


Fig. 19- Net-To-Gross Modelling for B9300, H1400, and J9400

The permeability models reveal a clear depth-dependent decline in reservoir flow capacity, with B9300 exhibiting high permeability, excellent lateral and vertical connectivity, and superior deliverability; H1400 showing moderate, facies-controlled permeability with increased heterogeneity and compartmentalization; and J9400 characterized by low permeability, shale-dominated architecture, poor connectivity, and highly restricted flow confined to isolated fault-bounded sand bodies (Fig. 20).

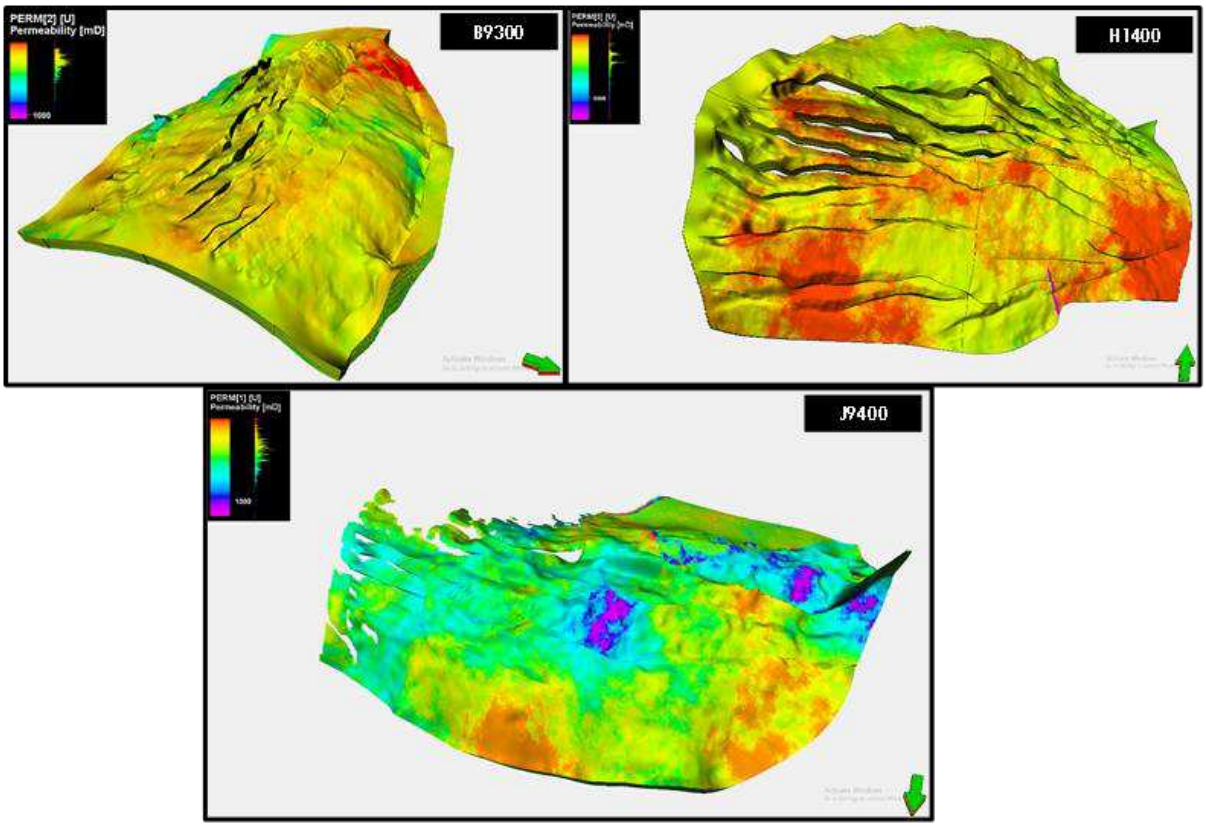


Fig. 20- Permeability Modelling for B9300, H1400, and J9400

Fluid contact modelling indicates a progressive decline in hydrocarbon trapping efficiency with depth, where B9300 contains a regionally consistent OWC, large connected hydrocarbon columns, and strong structural closure, H1400 exhibits compartmentalized hydrocarbon accumulations with variable column heights and fault-controlled fluid distribution, while J9400 is largely water-saturated with only small, isolated hydrocarbon pockets, reflecting poor trap development, strong aquifer influence, and limited reservoir potential (Fig. 21).

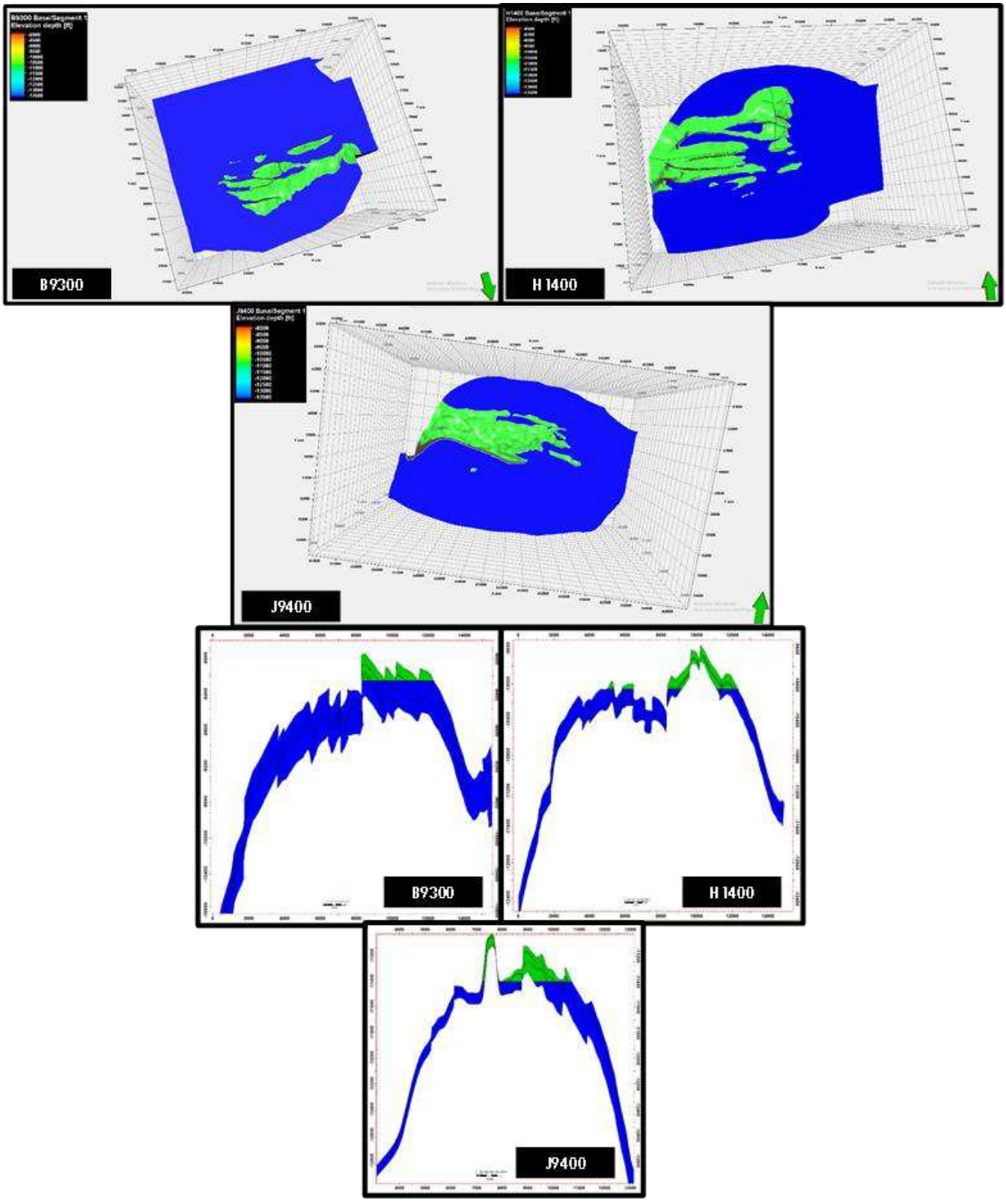


Fig. 21- Oil Water Contact for B9300, H1400, and J9400

4.0 Volumetric and Uncertainty Analysis

Volumetric analysis of the Albite Field reservoirs reveals significant differences in hydrocarbon potential and uncertainty across the three reservoir intervals. The B9300 reservoir contains an estimated STOIIP of approximately 475–551 MMstb (P50 ≈ 550 MMstb) and represents the most reliable reservoir, characterized by high porosity, low shale volume, high NTG, low water saturation, and excellent permeability. Although the H1400 reservoir contains the largest hydrocarbon volume (STOIIP ≈ 847–940 MMstb; P50 ≈ 860–900 MMstb), its reservoir quality and connectivity are reduced by increased shale content, fault compartmentalization, and facies heterogeneity, resulting in greater uncertainty and development risk. In contrast, the J9400 reservoir contains a relatively small hydrocarbon volume (STOIIP ≈ 252 MMstb; P50 ≈ 252 MMstb) and exhibits poor reservoir quality, low effective porosity, low NTG, high water saturation, and extensive shale development, which severely limit hydrocarbon storage and connectivity.

The uncertainty analysis shows that structural uncertainty is negligible across all reservoirs; B9300 is a low-risk, high-confidence reservoir with moderate petrophysical uncertainty (10–15%), H1400 has greater geological uncertainty due to facies heterogeneity and fault compartmentalization despite larger volumes, while J9400 is a geologically constrained, highly compartmentalized reservoir where uncertainty is dominated by connectivity and producibility rather than STOIIP variability.

Parameter	Case1	Case2	Case3
STOIIP (MMstb)	548.41	474.83	551.26
HCPV (MMRB)	762.29	660.01	766.26
Pore Volume (MMRB)	991.28	891.69	984.51
Net Volume (10^9 ft³)	18.68	16.88	18.62
Bulk Volume (10^9 ft³)	22.96	22.96	22.96

Fig. 22- Volumetric Analysis for B9300, H1400, and J9400

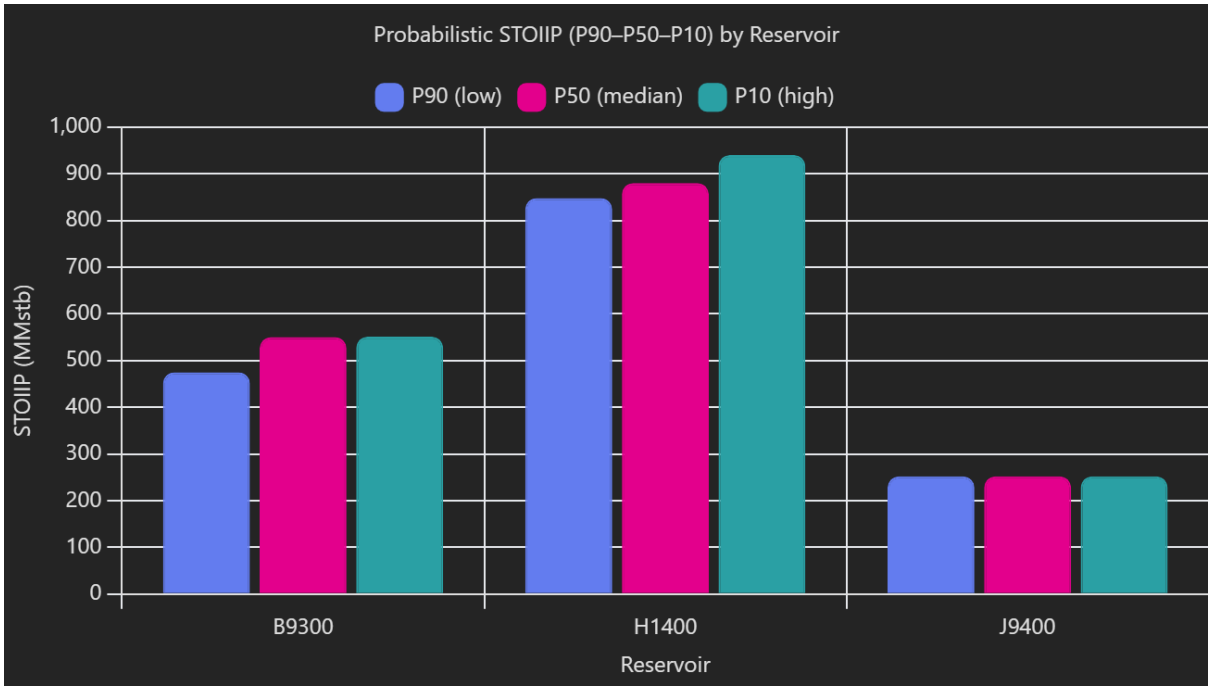


Fig. 23 Uncertainty Analysis for B9300, H1400, and J9400

5.0 Conclusion

An integrated reservoir characterization of the Albite Field combining seismic interpretation, depositional analysis, facies modelling, petrophysical modelling, fluid-contact analysis, volumetric estimation, and uncertainty assessment revealed a strong structural and depositional control on reservoir quality and hydrocarbon distribution. The field is dominated by growth-fault-related compartmentalization, while depositional environments evolve from a sand-rich fluvial system in B9300, through a heterogeneous fluvio-tidal system in H1400, to a marine-influenced, shale-dominated system in J9400. This vertical evolution results in increasing shale content, reduced porosity and permeability, lower net-to-gross ratios, higher water saturation, and poorer reservoir connectivity with depth.

Fluid-contact modelling confirms that hydrocarbon accumulations are primarily controlled by structural closure and fault compartmentalization, with B9300 containing the most extensive and well-connected hydrocarbon-bearing intervals, H1400 exhibiting compartmentalized accumulations with moderate connectivity, and J9400 containing only small, isolated hydrocarbon pockets.

Volumetric analysis estimated P50 STOIIP values of approximately 550 MMstb for B9300, 860–900 MMstb for H1400, and 252 MMstb for J9400. Although H1400 contains the largest in-place volume, its recoverable potential is reduced by greater heterogeneity and uncertainty.

Uncertainty analysis indicates that volumetric variability is controlled mainly by petrophysical parameters and reservoir connectivity, while structural uncertainty is negligible due to the well-constrained structural framework. Overall, B9300 is identified as the highest-quality and lowest-risk reservoir, H1400 as a volumetrically significant but moderately uncertain reservoir, and J9400 as a geologically constrained, high-risk reservoir with limited development potential, providing a robust basis for reservoir management and future field development planning.

AUTHORS CCONTRIBUTIONS

Obihan Ifeanyi contributed in conceptualization of the work, data processing, analysis and interpretation.; **Ologe Oluwatoyin** contributed in data processing and analysis; **Alege Tope. S** contributed in the interpretation: **Abdulbariu Ibrahim** contributed in processing and interpretation and **Ameloko Anthony A** contributed in interpretation and proof reading.

No funding

Ethics declaration: not applicable

References

Abiola, O., Olowokere, M.T., & Ojo, J.S. (2018). Sequence Stratigraphy and Depositional Sequence Interpretation: A Case Study of George Field, Offshore Niger Delta, Nigeria. *Petroleum Research*, 3(2), 123–136.

Avbovbo, A.A. (1978). *Tertiary Lithostratigraphy of the Niger Delta*. AAPG Bulletin, 62, 295–300.

Burke, K., (1972) Longshore rift, Submarine Canyons, and Submarine Fans in the development of Niger Delta, 56, American Association of Petroleum Geologists. pp. 289-291

Doust, H., & Omatsola, E. (1990). *Niger Delta*. In Edwards, J.D. & Santogrossi, P.A. (Eds.), Divergent/Passive Margin Basins, AAPG Memoir 48, 239–248.

Evamy, B.D., Haremboure, J., Kamerling, P., Knaap, W.A., Molloy, F.A., & Rowlands, P.H. (1978). Hydrocarbon Habitat of Tertiary Niger Delta. *AAPG Bulletin*, 62, 277–298.

Ikomi, M. K. and Nfor, B. N. (2021). Petrophysical Evaluation of Reservoirs of the X-Field, offshore, Niger Delta, Nigeria. *IOSR Journal of Applied Geology and Geophysics (IOSR-JAGG)*, 9(5), 55-61.

Nton, M.E., & Rotimi, S. (2016). Reservoir Characteristics and Palaeo-Depositional Environment of Duski Field, Onshore Niger Delta, Nigeria. Global Journal of Geological Sciences.

Obaje, N.G (2009). The Niger Delta Basin. In: Geology and Mineral Resources of Nigeria. Lecture Notes in Earth Sciences, 120, Springer, Berlin, Heidelberg. 10.1007/978-3-540-92685-6_10

Tsimitakopoulos K. (2022). The Niger Delta Basin: Reform has Finally Come, but can it Revive Investment in the Oil and Gas Sector? S&P Global Commodity Insights. 〈 https://www.spglobal.com/commodityinsights/en〉

Short, K.C., & Stauble, A.J. (1967). Outline of Geology of Niger Delta. *AAPG Bulletin*, 51, 761–779.

Tuttle, M.L.W., Brownfield, M.E., & Charpentier, R.R. (1999). *The Niger Delta Petroleum*

System. USGS Open File Report 99-50H